



# Identification of 12 hub genes associated to the pathogenesis of osteoporosis based on microarray and single-cell RNA sequencing data

Zhigang Zhou<sup>1,2</sup> · Zhangheng Huang<sup>1</sup> · Haider Mohammed Khan<sup>1</sup> · Yuheng Liu<sup>1</sup> · Zhen Zhao<sup>1</sup> · Qingquan Kong<sup>1</sup>

Received: 10 March 2023 / Revised: 12 May 2023 / Accepted: 18 May 2023 / Published online: 27 May 2023  
© The Author(s), under exclusive licence to Springer-Verlag GmbH Germany, part of Springer Nature 2023

## Abstract

Osteoporosis is a common disease, especially among the elderly. This study aimed to comprehensively examine the roles of immune microenvironment in osteoporosis pathogenesis. Expression profiles of GSE35959, GSE7158, and GSE13850 datasets were used to analyze differential expression and identify hub genes related to immune features. Based on the single-cell RNA sequencing (scRNA-seq) data of an osteoporosis patient, different cell types were classified and the relation between immune environment and osteoporosis was explored. Twelve hub genes significantly associated with immune features were selected and 11 subgroups were defined using scRNA-seq data. The expression of two hub genes (*CDKN1A* and *TEFM*) was greatly altered during the transformation from mesenchymal stem cells (MSCs) to osteoblasts. Chemokines and chemokine receptors were differentially enriched in different cell types. *CXCL12* was high-expressed in MSCs. This study emphasized that immune microenvironment played a critical role in the pathogenesis of osteoporosis. Chemokines and chemokine receptors can modify cell development and affect the interactions among different cell types, leading to unbalanced bone remodeling.

**Keywords** Osteoporosis · Immune microenvironment · Chemokines · Mesenchymal stromal cells · Osteoblasts · Bone remodeling

## Introduction

Osteoporosis, a metabolic disease, is mainly characterized by reduced bone mass, can cause bone structure alternation and fractures. An estimated 200 million patients suffer from osteoporosis worldwide (Akkawi and Zmerly 2018). Aging is a common risk factor for osteoporosis, and approximately over 30% people, particularly post-menopausal women, will experience an osteoporosis-caused fracture in their late live (Sözen et al. 2017). Other important risk factors such as abnormal hormone function, low body mass index, races, low body mineral density (BMD), and deficiency of vitamin

D can also affect the occurrence or severity of osteoporosis (Qaseem et al. 2017).

Imbalance between bone reabsorption by osteoclasts and bone formation by osteoblasts is a direct factor leading to abnormal bone remodeling that could subsequently affect bone shaping and bone fractures. During the process of bone remodeling, evidence demonstrated that macrophage colony-stimulating factor (M-CSF) and its receptor c-fms, receptor activator of NF- $\kappa$ B ligand (RANKL) and its receptor RANK are involved in regulating osteoblasts (Li et al. 2021), suggesting that signaling pathways could be potential targets for osteoporosis treatment. Denosumab has been approved by the Food and Drug Administration (FDA) as an effective drug to treat osteoporosis through competitively bonding with RANKL (Cummings et al. 2009). Mesenchymal stem cells (MSCs) are recognized as progenitor of osteoblasts and could differentiate into many cell types. Transcript factors of *runx2*, *osterix*, and  $\beta$ -catenin are involved in osteoporosis differentiation (Komori 2006). Currently, there is no clinically effective drug for targeting osteoblasts, which requires in-depth study probing into the mechanisms of osteoblasts in regulating bone remodeling.

✉ Qingquan Kong  
kqqspine@126.com

<sup>1</sup> Department of Orthopedics Surgery, West China Hospital, Sichuan University, Orthopedic Research Institute, West China Hospital, Sichuan University, No. 37 Guo Xue Lane, Chengdu 610041, Sichuan, China

<sup>2</sup> Department of Spine Surgery, Jiujiang No. 1 People's Hospital, Jiujiang, China

In the development of osteoporosis, immune cells play important roles. It has been observed that activated T lymphocytes-produced TNF- $\alpha$  contributes to bone destruction and bone loss via activating RANKL and M-CSF in mice model (Cenci et al. 2000; Kong et al. 1999). A series of T helper (Th) cells are responsible for the pathogenesis of osteoporosis through secreting cytokines and chemokines to modulate immune microenvironment (Collins et al. 2017; Koizumi et al. 2009; Srivastava et al. 2018). Cytokines IL-4, IL-5, and IL-13 secreted from Th2 cells are implicated in the inhibition of osteoclastogenesis (Palmqvist et al. 2006). Th17 cells can enhance osteoclastogenesis through secreting high levels of IL-1, IL-6, IL-17, RANKL, and TNF (Dar et al. 2018). In addition, natural killer cells, regulatory T cells,  $\gamma\delta$ -T cells and CD8 T cells have been found to modulate osteoporosis development (Srivastava et al. 2018). Collectively, immune microenvironment plays an essential role in regulating bone remodeling. However, critical genes associated with immune cells in osteoporosis development have not been discovered.

Weighted correlation network analysis (WGCNA), which describes gene association patterns among different samples (Langfelder and Horvath 2008), can be used to identify highly variable gene sets and candidate biomarker genes or therapeutic targets based on the interconnectivity of gene sets and the association between the gene sets and phenotype (Pei et al. 2017).

In this work, we produced a co-expression network based on differentially expressed genes between normal samples and osteoporosis samples, and identified several hub genes related to immune features. Single-cell RNA sequencing (scRNA-seq) data were employed to define different cell types and characterize their function for revealing the pathogenesis of osteoporosis.

## Methods

### Data source and data preprocessing

Normal samples, osteoporosis samples, and their chip expression data (GSE35959, GSE7158 and GSE13850) were obtained from Gene Expression Omnibus (GEO, <https://www.ncbi.nlm.nih.gov/geo/>) database. GSE35959 (5 normal samples and 5 osteoporosis samples) included the expression profile of mesenchymal stem cell populations from elderly patients (79 to 94 years old) with osteoporosis. Mesenchymal stem cells are the primary source of osteogenic regeneration. GSE7158 (14 normal samples and 12 peak bone mass samples) was a microarray profile of circulating monocytes in human subjects with peak bone mass that has been reported to be an important determinant of osteoporosis. GSE13850 (20 normal samples

and 20 osteoporosis samples) contained the expression profiles of circulating B cells from postmenopausal females with smoking-related osteoporosis. The sample information of 3 datasets was shown in Table 1. For the three datasets, samples without clinical follow-up information, survival status, or survival time were removed, and the probe number was converted into Gene symbol. When multiple probes matched a gene, the mean value was taken as the expression value of the gene. The expression of the gene missing in 80% of cases was excluded for each dataset. Principle component analysis (PCA) was used to remove heterogeneity among the three datasets through conducting “removeBatchEffect” function in sva R package. After removing heterogeneity, the data were adjusted by “normalizeBetweenArrays” function in limma R package. PCA plots showed no difference among samples from different datasets (Supplementary Figure S1).

### Single-cell RNA sequencing data

The scRNA-seq data (GSE147287) were downloaded from GEO. The RNA data containing an osteoporosis sample and an osteoarthritis sample was sequenced by 10 $\times$  sequencing platform. This study only included osteoporosis sample (ID: GSM4423510), the single-cell data of which were used to analyze different subgroups with distinct signatures and cell trajectory.

### Enrichment analysis of immune cells

CIBERSORT (<http://cibersort.stanford.edu/>) is an analytical tool for estimating the abundances of member cell types in a mixed cell population (Chen et al. 2018) used in this study to calculate the enrichment score of 22 immune cells in 39 normal samples and 37 osteoporosis samples. Wilcoxon test was performed to analyze significance that was defined at  $p < 0.05$ .

**Table 1** The samples of 3 datasets

Datasets	Samples	Numbers
GSE13850	High_PBM	20
	Low_PBM	20
GSE35959	no_Osteoporosis	5
	Osteoporosis	5
GSE7158	High_PBM	14
	Low_PBM	12

## Weighted gene correlation network analysis

The preprocessed data of 76 samples were included to screen differentially expressed genes using limma R package (Diboun et al. 2006) under the criterion of  $p < 0.05$ . Then we applied weighted gene correlation network analysis (WGCNA) to produce a co-expression network based on the differentially expressed genes. WGCNA is a widely used to explore co-expressed genes and gene modules and to associate gene expression data with other molecular features or phenotypes (Langfelder and Horvath 2008). To examine whether a similar expression pattern was present between the two genes, Pearson correlation rank analysis was performed to calculate gene distance. Power of software threshold ( $\beta$ )  $> 0.85$  ensured a scale-free network and confirmed co-expression gene modules. Then, a dendrogram based on the correlation coefficients between genes was developed using hierarchical clustering. A series of gene modules were excavated, according to the dynamic cutting criterion of at least 30 genes in a branched network. Eigengenes of each gene module were calculated, and similar modules were aggregated under  $\text{height} = 0.25$ ,  $\text{deepSplit} = 2$ ,  $\text{minModuleSize} = 30$ . Finally, we obtained five modules and analyzed the correlation between modules and immune features.

## Screening hub genes and functional analysis

Pearson correlation analysis was applied to calculate the correlation coefficient between gene modules and target cell groups. According to the correlations between eigengene of modules and gene expression profiles (MM), gene expression and the enrichment of target cell groups (GS),  $\text{MM} > 0.8$  and  $\text{GS} > 0.5$  were set to filter hub genes in the module. WebGestalt R package was employed to annotate Gene Ontology (GO) terms and Kyoto Encyclopedia of Genes and Genomes (KEGG) pathways (Liao et al. 2019) of the hub genes screened.

## Dimensional reduction analysis for identifying cell subgroups and cell trajectory

Single-cell data of an osteoporosis sample (ID: GSM4423510) were preprocessed by Seurat R package (Butler et al. 2018) and then used to identify cell subgroups. Single-cell data were filtered under the conditions that each gene was expressed at least in 3 cells and each cell contained the expression of at least 250 genes. “PercentageFeatureSet” function was used for calculating the proportion of mitochondria and rRNA under the condition that each cell expressed at least 500 genes with no more than 30% mitochondria. Totally 5881 cells and 20,433 genes were included for further analysis. The quality control plot before and after the filtration was shown. Then “NormalizeData” function

and “FindVariableFeatures” function were used to normalize the data and detect highly variable genes, respectively. “ScaleData” function was applied to reduce high-dimensional data into a two-dimensional diagram. Next, we used the functions of “FindNeighbors” and “FindClusters” and set  $\text{dim} = 30$  to cluster cells into 11 cell subgroups. “FindAllMarkers” function with  $\text{logfc} = 0.5$ , and  $\text{Minpct} = 0.25$  was used to screen marker genes from the 11 subgroups. To further define the 11 subgroups, marker genes of bone marrow and bone from CellMarker (<http://biocc.hrbmu.edu.cn/CellMarker/>) were downloaded and “enricher” function in clusterProfiler R package was used to define these subgroups (Yu et al. 2012). Monocle R package was applied to assess cell development and trajectory (Qiu et al. 2017).

## Enrichment of functional pathways for scRNA-seq data by ReactomeGSA

Reactome (Home-Reactome Pathway Database) is an open-source enrichment analysis database. ReactomeGSA R package operates a multi-omics analysis across species for scRNA-seq data (Griss et al. 2020) and can be directly linked to Reactome database (<https://reactome.org/>) with comprehensive pathways. This tool was used here to enrich the functional pathways for each subgroup, and the top 10 differentially enriched pathways were selected.

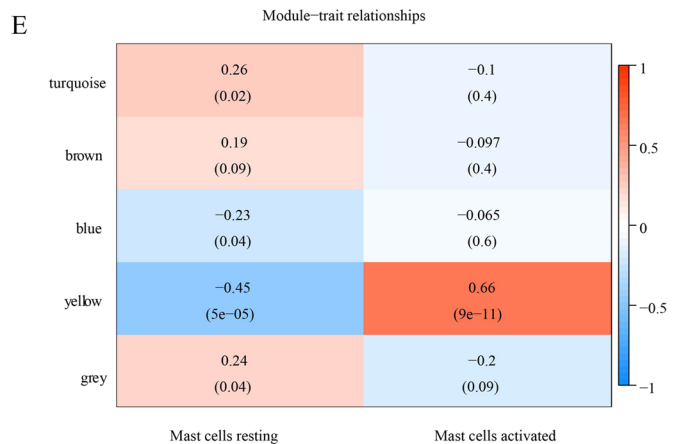
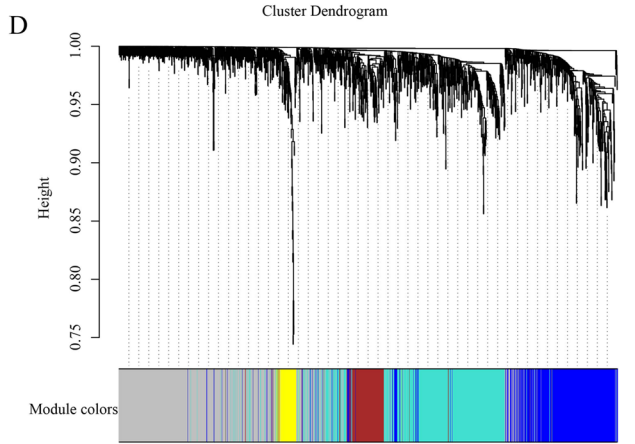
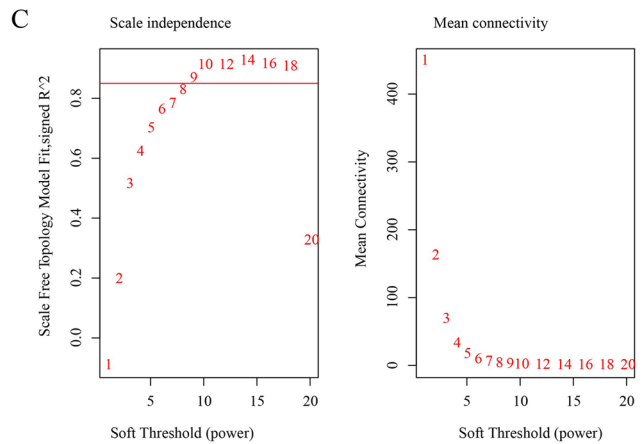
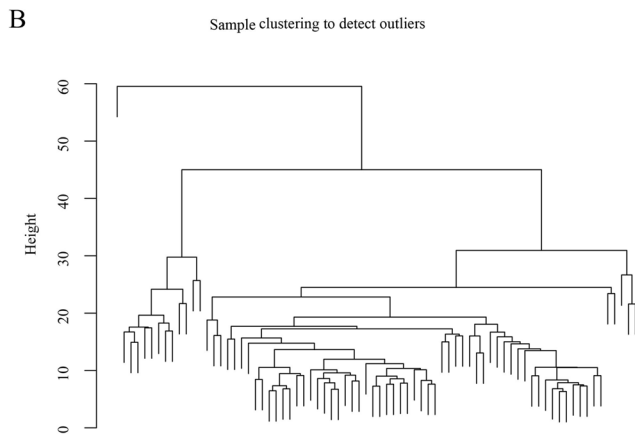
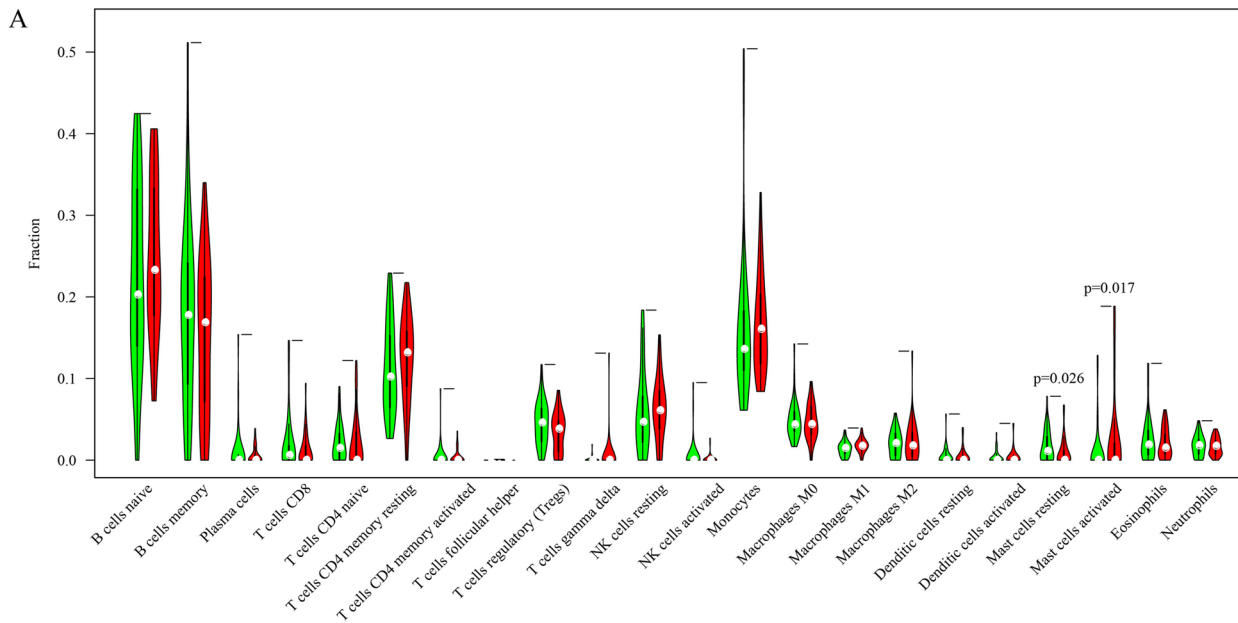
## Statistical analysis

All the statistical analysis were performed in R platform (v.3.4.2). Specific statistical methods were described in the figure legends. The parameters not mentioned were default in packages.  $P < 0.05$  was considered as significant.

## Results

### Identification of gene modules associated with immune features in osteoporosis samples

To examine whether there was a difference of immune cell distribution between 39 normal samples and 37 osteoporosis samples, CIBERSORT was used to measure the enrichment of 22 immune cells. Among these immune cells, only resting mast cells and activated mast cells showed a difference between normal samples and osteoporosis samples ( $P = 0.026$  and  $P = 0.017$  respectively, Fig. 1A). This indicated that mast cells may play an important role in the development of osteoporosis. To further identify the genes responsible for aberrant proportion of mast cells in osteoporosis samples, we applied WGCNA to develop a co-expression gene network and classified gene modules associated with immune features. Based on the expression profiles of



1722 differential expressed genes, hierarchical clustering was conducted (Fig. 1B). Power of soft threshold ( $\beta$ )=9 was selected to meet a scale-free topology (Fig. 1C). According to the topology matrix, average-linkage hierarchical clustering and dynamic cutting standard were employed to cluster

genes under the condition that each gene cluster contained at least 30 genes. Then gene clusters were further combined to gene modules based on eigengenes of gene clusters, and finally five gene modules were identified (Fig. 1D). Pearson correlation analysis between gene modules and immune

**Fig. 1** Identification of gene modules significantly correlated with mast cells. **(A)** The distribution of 22 immune cells in 39 normal samples (green) and 37 osteoporosis samples (red) analyzed by CIBERSORT. Wilcoxon test was performed. **(B)** Hierarchical clustering for 76 samples based on differential gene expression. **(C)** Scale-free topology model fitting ( $R^2$ ) and mean connectivity for determining the optimal power of soft threshold ( $\beta=1$  to 20). Red line indicates  $R^2=0.85$ . **(D)** Clustering of gene dendrogram based on eigengenes and at least 30 genes in one cluster. Turquoise, brown, blue, yellow, and grey represent different gene modules after clustering. Grey module is a cluster where genes cannot be aggregated into other gene modules. **(E)** Pearson correlation analysis between gene modules and the distribution of mast cells. Orange indicates positive correlation and blue indicates negative correlation. Numbers without brackets indicate the correlation coefficient and numbers with brackets indicate  $P$  values

features (resting and activated mast cells) revealed that the yellow gene module was closely related to the distribution of resting mast cells ( $R=-0.45$ ,  $P=5e-05$ ) and activated mast cells ( $R=0.66$ ,  $P=9e-11$ , Fig. 1E). The results indicated that hub genes were present in the yellow gene module and may affect the enrichment of mast cells via potential pathways.

### An interaction network of 12 hub genes responsible for osteoporosis

As the yellow gene module was verified to be closely associated with the enrichment of mast cells, we then excavated hub genes involved in osteoporosis. We screened 12 hub genes when  $MM > 0.8$  and  $GS > 0.5$  based on the correlations between eigengene of yellow module and gene expression profiles (module membership in the yellow module,  $MM$ ), gene expression and the enrichment of activated mast cells (gene significance for activated mast cells,  $GS$ ) (Fig. 2A). A protein–protein interaction (PPI) network containing 65 genes within the yellow module was developed, with blue indicating downregulated genes and red indicating upregulated genes (Fig. 2B). A total of 12 genes (*CD83*, *CDKN1A*, *GADD45B*, *ICAM1*, *JUNB*, *NLRP3*, *PLAUR*, *PPP1R15A*, *PTGS2*, *RIPK2*, *MRFAP1L1*, and *TEFM*) located in the center of the network. These 12 genes were taken into the consideration as potential hub genes potentially involved in regulating mast cells and the pathogenesis of osteoporosis. The correlation analysis between the 12 hub genes and activated mast cells, as well as resting mast cells, showed that the 12 hub genes were associated to the two immune cells (Fig. 2C). Enrichment analysis on 65 genes annotated 367 terms of biological processes (top 10 terms in Fig. 2D), 4 terms of molecular functions (Fig. 2E), 0 term of cellular component and 15 KEGG pathways (top 10 pathways in Fig. 2F) ( $P < 0.05$ ).

Subsequently, we detected the expression of 12 hub genes in normal samples and osteoporosis samples, and the

result showed that *CD83*, *CDKN1A*, *GADD45B*, *ICAM1*, *JUNB*, *NLRP3*, *PLAUR*, *PPP1R15A*, *PTGS2*, and *RIPK2* were higher-expressed in osteoporosis samples, while *MRFAP1L1* and *TEFM* were relatively higher-expressed in normal samples ( $P < 0.05$ , Fig. 2G). Interestingly, Pearson correlation analysis on the 12 hub genes showed that both the expressions of *MRFAP1L1* and *TEFM* were negatively correlated with other 10 genes (Fig. 2H).

### Identifying 11 immune cell subgroups in osteoporosis based on single-cell data and dimensional reduction analysis

Next, we explored the developing process of osteoporosis at a molecular level using gene expression analysis of each cell with single-cell RNA sequencing data of the osteoporosis sample (ID: GSM4423510). The first filtration was performed under criteria that each gene expressed in at least three cells and each cell expressed at least 250 genes. Then under the threshold that each cell expressed in at least 500 genes and the proportion of mitochondria was fewer than 30%, a final total of 5881 cells and 20,433 genes were included for further analysis (Supplementary Figure S2). Subsequently, we assessed the distribution of highly variable genes and non-variable genes, and the top 20 highly variable genes were annotated (Supplementary Figure S3). PCA was performed to generate a two-dimensional distribution according to the expression of all genes (Supplementary Figure S4). Marker genes of each subgroup were screened, and the expression of the top 5 marker genes from each subgroup was presented (Supplementary Figure S5). Eleven subgroups displayed a significantly differential expression of these marker genes, validating the effectiveness and reliability of the subgrouping.

Markers genes of bone and bone marrow downloaded from CellMarker (<http://biocc.hrbmu.edu.cn/CellMarker/>) were used to define the 11 subgroups. The result showed that the 11 subgroups corresponded to different types of cells, except for subgroups 2, 3, and 10 that belonged to the same cell lineage of lymphoid-primed multipotent progenitor (LMPP) (Fig. 3A). Comparison of these three subgroups demonstrated that subgroup 2 specifically expressed *LCN2*, *LTF*, and *CAMP*, subgroup 3 specifically expressed *CD14*, and subgroup 10 specifically expressed *DNTT*, *VPREB1* and *IGLL1* (Fig. 3B). Furthermore, the cell trajectory of each subgroup was visualized by monocle to characterize cell development (Fig. 3C and D). It could be observed that MSCs located in the early pseudotime, while plasmacytoid dendritic cells located in the late pseudotime. Noticeably, MSCs, mast cell progenitor, and osteoblasts almost located in the same branch.

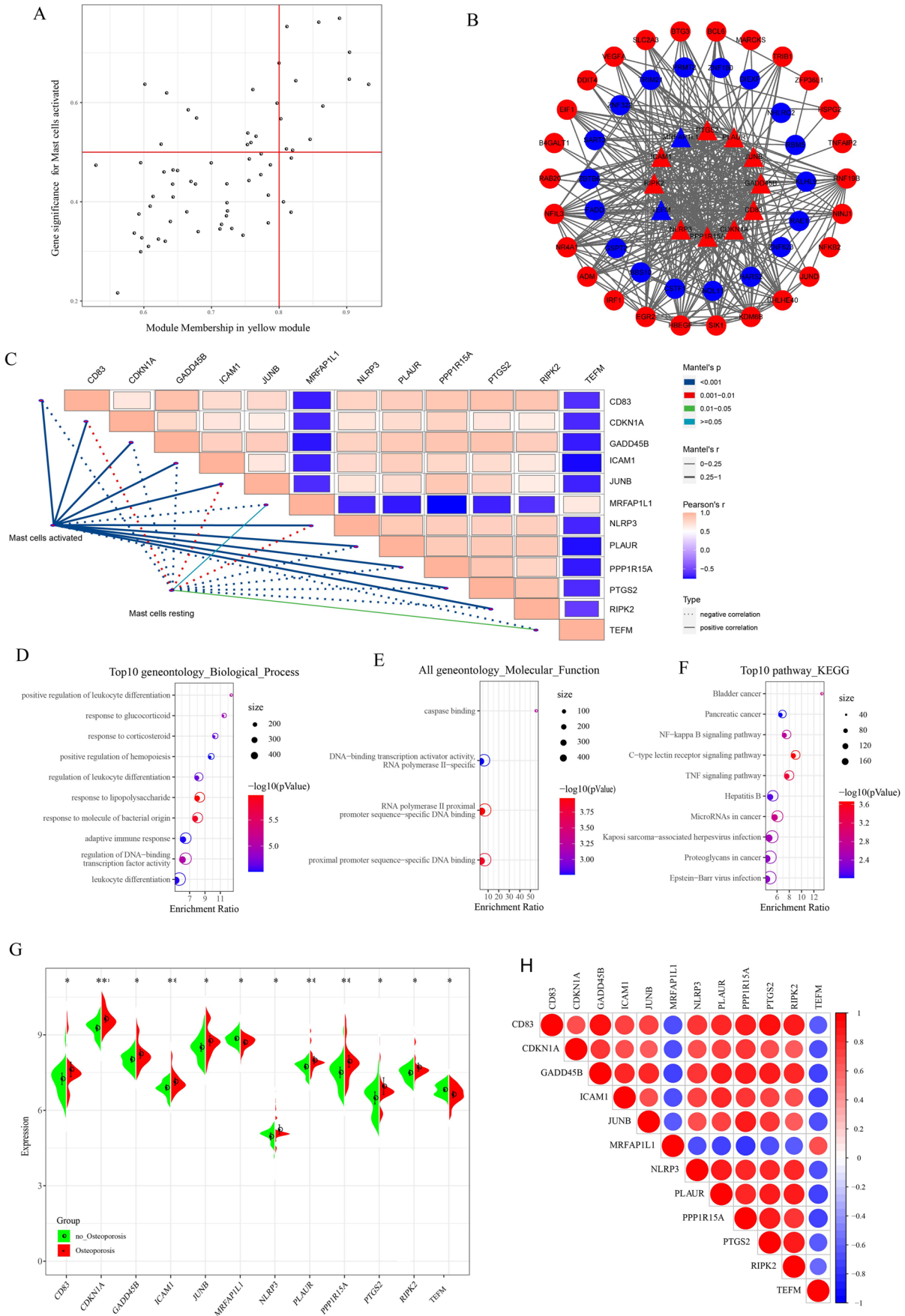


**Fig. 2** Screening of 12 hub genes associated with osteoporosis. (A) Screening hub genes in yellow module with conditions  $MM > 0.8$  and  $GS > 0.5$  indicated by red lines. (B) The gene–gene interaction network of genes in yellow module. Triangles represent hub genes. Circles represent other genes in yellow module. Red indicates upregulated genes and blue indicates downregulated genes. (C) The correlation analysis of 12 hub genes and mast cells. (D–F) The top 10 annotate terms of biological process (D), molecular function (E), and KEGG pathways (F). Annotated terms that less than 10 were all presented. Dot size indicates the number of enriched genes.  $P$  value was presented as  $-\log_{10}(P \text{ value})$ . (G) Comparison of hub gene expression between normal (red) and osteoporosis (green) samples. Student  $t$  test was performed. (H) Pearson correlation analysis among 12 hub genes. Red indicates positive correlation and blue indicates negative correlation. \* $P < 0.05$ , \*\* $P < 0.01$ , \*\*\* $P < 0.001$

## Differential gene expression signatures and immune features of 11 subgroups

In the previous section, we identified 12 hub genes markedly associated with activated mast cells. Here we analyzed the expression level of 12 hub genes in the 11 subgroups to clarify potential regulation of the hub genes on cell development of osteoporosis (Fig. 4A). Mesenchymal stromal cells could differentiate into various cell types such as osteoblasts, and can modulate immune response through silencing or activation themselves. We found that *CD83* was high-expressed in myeloid cells and B cells. *GADD45B* was more expressed in plasmacytoid dendritic cells. *ICAMI*, *PLAUR* and *RIPK2* were activated in myeloid cells, and *JUNB* was significantly activated in LMPP 1 and 2. *MRFAP1L1* was activated in lymphocytes and LMPP 3. *PPP1R15A* was found to be markedly activated in plasmacytoid dendritic cells and high-expressed in mast cell progenitor. *PTGS2* was activated in LMPP 1, and *TEFM* was all suppressed in other cell types compared with mesenchymal stromal cells.

To assess their functional pathways of 11 subgroups, we applied ReactomeGSA R package for functional enrichment analysis. The top 10 differentially enriched pathways were presented (Fig. 4B and Supplementary Figure S6). Difference among LMPP 1, 2, and 3 could be clearly observed. Similar enrichment patterns between LMPP 1 and mesenchymal stromal cells were observed. FGFR3b ligand binding and activation pathways, and sterols 12-hydroxylated by CYP8B1 pathway were more enriched in osteoblasts (Fig. 4C). However, the pathway of activation of Na-permeable kainate receptors was strongly suppressed. In mast cell progenitor, significantly high enrichment of Rhesus blood group biosynthesis was found.

Previous studies showed that chemokines and chemokine receptors play important roles in bone formation and destruction (Collins et al. 2017; Koizumi et al. 2009; Pathak et al. 2015). We therefore obtained 41 chemokines and 18 chemokine receptors from a previous literature (Ru et al. 2019), and analyzed their expression level in the 11

subgroups (Fig. 4D). The result indicated that the proportion of CXCL12 expression was a high in all the cell types. Specifically, CXCL12 had the highest expression in mesenchymal stromal cells but a significantly low expression in other cell types. A majority of osteoblasts still expressed CXCL12, but its expression was a relatively low when compared with mesenchymal stromal cells. LMPP 1, 2, and 3 still presented a marked difference, specifically, CCR1 and CCR2 had the highest expression in LMPP 2, and CXCR4 was high-expressed in LMPP 1. Lymphocytes mostly expressed CCL4 and CCL5, and myeloid cells showed a high expression of CXCL16 and CCR1. The differential distribution of chemokines and chemokine receptors in different subgroups supported the important roles of different cell types in secreting specific chemokines or chemokine receptors, which may regulate the formation of osteoblasts and osteoclasts.

## Discussion

Comparison of immune microenvironment between normal samples and osteoporosis samples showed that only resting mast cells and activated mast cells were differentially distributed, indicating the potential importance of mast cells. Previous studies also revealed the important role of mast cells in osteoporosis pathogenesis. Low or high numbers of bone marrow mast cells are considered to be associated with bone remodeling, and increased mast cells are frequently discovered in osteoporotic postmenopausal women and osteoporotic men (Brumsen et al. 2002). Chiappetta et al. reported that a great proportion of mast cells are responsible for facilitating bone turnover and pathogenesis of bone remodeling (Chiappetta and Gruber 2006). A study of indolent systemic mastocytosis (ISM) also supports the above conclusion that ISM patients, especially male patients, face a higher risk of osteoporotic fractures (van der Veer et al. 2012). Therefore, with a focus on mast cells, we screened a series of hub genes closely correlated with mast cells with WGCNA and Pearson correlation analysis.

Apart from *MRFAP1L1* and *TEFM*, the remaining 10 hub genes (*CD83*, *CDKN1A*, *GADD45B*, *ICAMI*, *JUNB*, *NLRP3*, *PLAUR*, *PPP1R15A*, *PTGS2*, and *RIPK2*) were all higher-expressed in osteoporosis samples. Among these hub genes, *CDKN1A*, *ICAMI*, and *NLRP3* have been previously reported to be closely related to the pathogenesis of osteoporosis. Cyclin-dependent kinase inhibitor 1A (*CDKN1A*) is high-expressed in bone samples from the elderly and has been considered as an important mediator for senescence to promote bone loss (Farr et al. 2019; Liu et al. 2015). Intercellular adhesion molecule-1 (*ICAMI*) expressed at the surface of osteoblasts can interact with its receptor expressed in osteoclasts, which is critical for maintaining

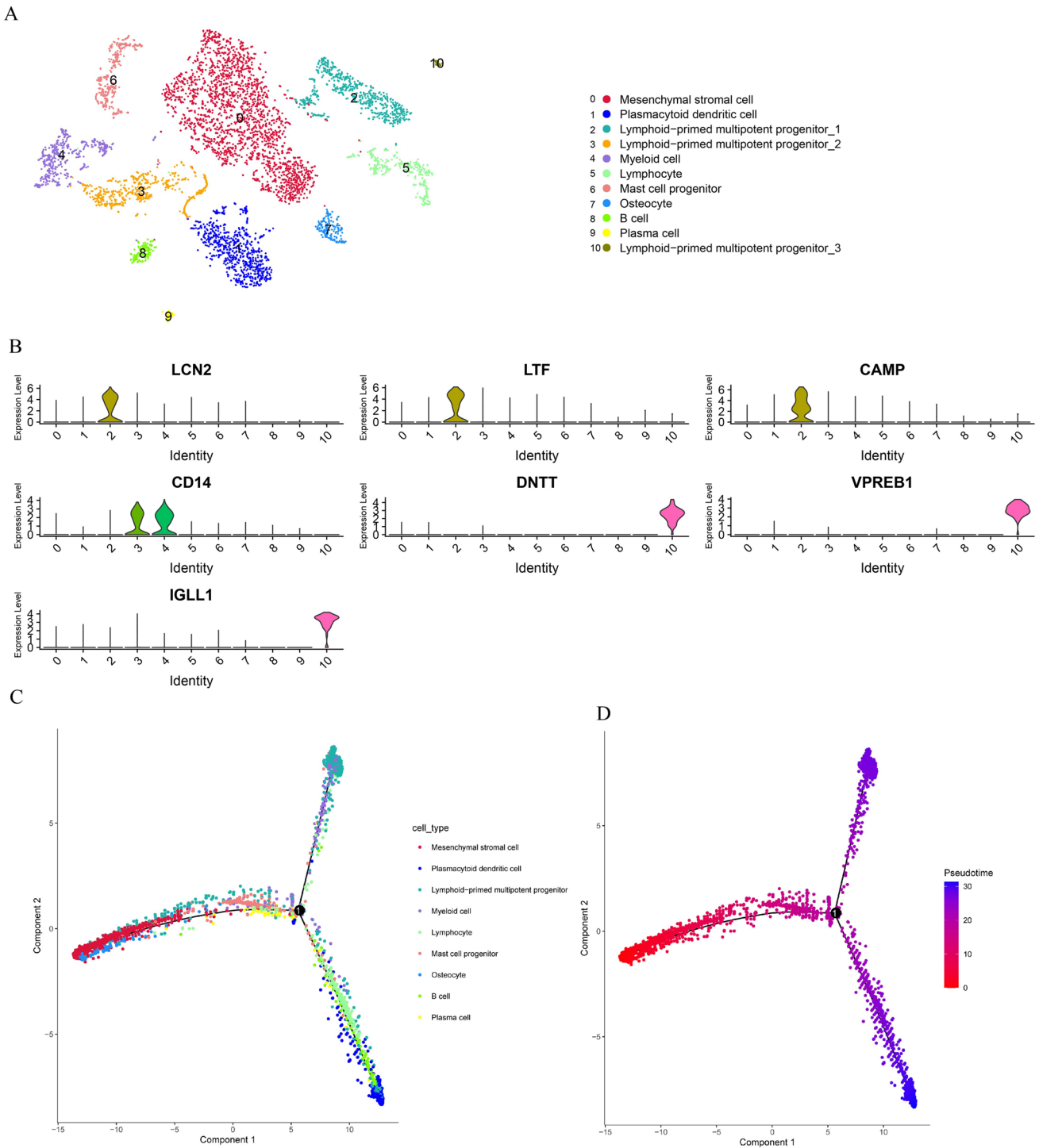


**Fig. 3** Definition of 11 subgroups and cell trajectory. **(A)** T-distributed stochastic neighbor embedding (t-SNE) plots for defining 11 subgroups into different cell types based on marker genes from CellMarker. **(B)** Violin plots of the specifically expressed marker genes (*LCN2*, *LTF*, *CAMP*, *CD14*, *DNNT*, *VPREB1*, *IGLL1*) in lymphoid-

primed multipotent progenitor 1, 2, 3. Horizontal axis represents 0 to 10 subgroups. **(C, D)** The cell trajectory of 9 cell types generated by monocle. The pseudotime from left to right indicates the predicted development time of cell types from early to late

bone homeostasis. In osteoporosis patients, an upregulated expression of ICAM1 is commonly observed (Lavigne et al. 2004). In addition, ICAM1 is regarded as a potential target

for controlling bone pathogenesis (Kong and Yang 2020; Lavigne et al. 2005). Pyrin domain containing protein 3 (NLRP3) is an inflammasome and its activation in MSCs



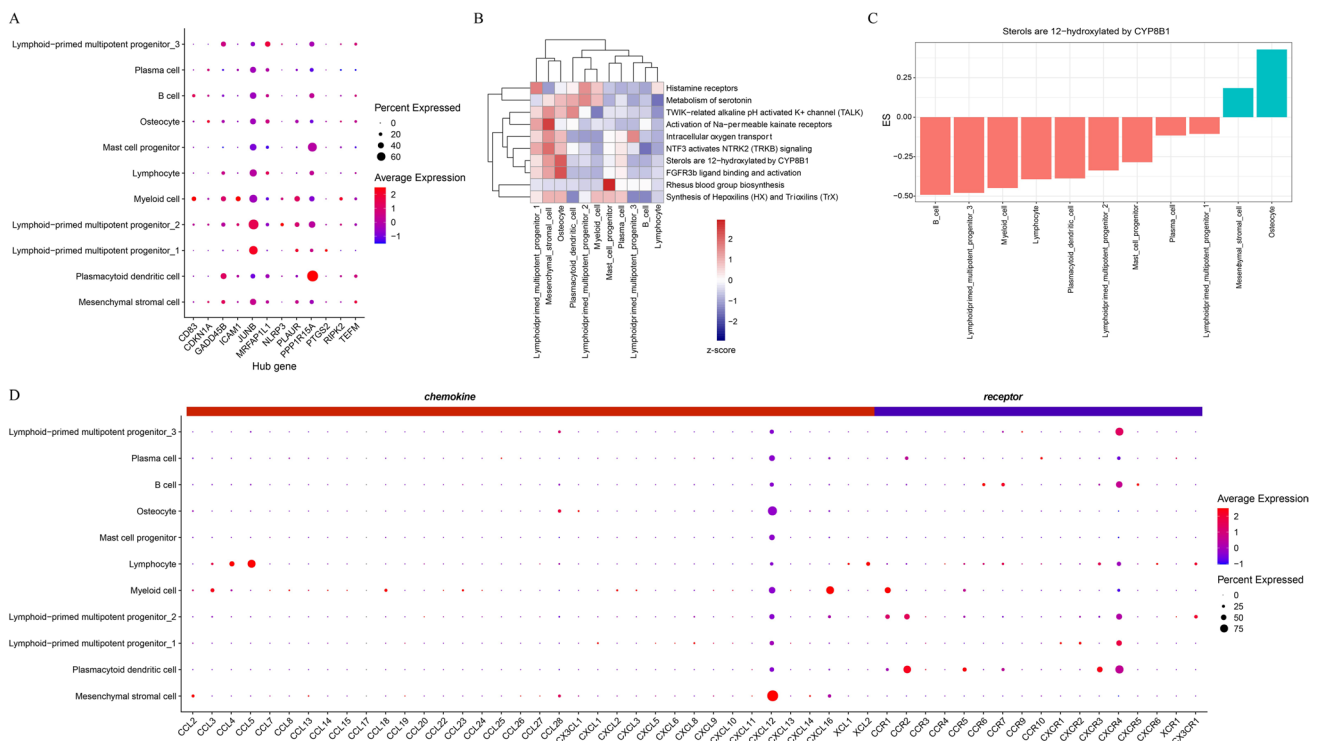


**Fig. 4** Delineating the expression signatures of 11 subgroups. **(A)** The expression patterns of 12 hub genes described as z-score in 11 subgroups. Dot size indicates the percentage of expressed cells in one cell type. Red indicates relatively high expression and blue-violet indicates relatively low expression. **(B)** The top 10 differentially enriched pathways of 11 subgroups. Red indicates relatively high enrichment score and blue indicates relatively low enrichment score.

**(C)** The enrichment score of sterols is 12-hydroxylated by CYP8B1 pathway in 11 subgroups. ES, enrichment score. **(D)** The expression of chemokines and chemokine receptors in 11 subgroups. Dot size indicates the percentage of expressed cells in one cell type. Red indicates relatively high expression and blue-violet indicates relatively low expression

can reduce osteogenesis from MSCs (Wang et al. 2017; Xu et al. 2018). The mutation of NLRP3 could cause osteoporosis in *Nlrp3*-mutant mice model (Snouwaert et al. 2016). Although other hub genes have not been demonstrated to have a significant correlation with osteoporosis, they still had the potential in further exploration of the mechanisms of osteoporosis pathogenesis. Notably, all these hub genes have not been reported to interact with mast cells, and our identification may unveil the mechanism of immune cells in the modulation of bone pathogenesis.

Next, we classified cell types in bone tissue with osteoporosis through assessing scRNA-seq data. Nine cell types and 11 subgroups were identified based on a large proportion of MSCs. MSCs can differentiate into osteoblasts, nerve cells, blood cells, liver cells, muscle cells, etc. in activated micro-environment. For the elderly, reduced number of MSCs and unbalanced bone-fat would weaken the ability of MSCs to generate sufficient number of osteoblasts (Ganguly et al. 2017). To some extent, bone physiology is involved in the pathogenesis of osteoporosis, but the formation of osteoporosis is induced by a diversity of factors that co-affect each other. In the process from MSCs to osteoblasts, we

observed significant alternation of four genes (*GADD45B*, *JUNB*, *PLAUR*, and *TEFM*) on both expressed cell numbers and expression level, indicating that the four genes may play important roles in the transformation (Fig. 4A).

Chemokines are a type of essential inflammatory mediators that assist bone modeling and participate in the pathogenesis of osteoporosis. Evidence has proven that CCL2 and CCR2 are elevated in osteoporosis patients, and that knockout of CCR2 inhibits the function of osteoclasts (Binder et al. 2009; Fatehi et al. 2017). This study found that CCL2 was high-expressed in MSCs and myeloid cells, and that CCR2 was high-expressed in plasmacytoid dendritic cells and LMPP 2 (Fig. 4D), indicating that immune cells secreting chemokine receptors could serve as an activator in promoting osteoporosis. CCL3, CCL4, and CCL5 expressions are upregulated in osteoporosis patients (Fatehi et al. 2017; Wan et al. 2018), but in our results, they were secreted majorly by lymphocytes. CCL20/CCR6 signaling could affect osteoblasts, and knock out of either of them in mice can reduce bone mass (Doucet et al. 2016). In the current work, CCL20 was enriched in LMPP 2 and CCR6 was enriched in B cells, further

indicating that immune microenvironment played a critical role in bone remodeling. CX3CL1 was mostly expressed in osteoblasts, and studies have presented that CX3CL1 is expressed by osteoblasts to interact with its receptor CX3CR1 on osteoclast progenitors (Han et al. 2014; Koizumi et al. 2009). Evidence also supported that CX3CL1 promotes bone loss mediated by osteoclasts (Han et al. 2014; Imai and Yasuda 2016).

CXCL12/CXCR4 signaling is considered as an essential pathway in regulating both osteoblast differentiation and osteoclast formation (Brylka and Schinke 2019). Tzeng et al. revealed that CXCL12 secreted by MSCs can regulate osteogenesis and adipogenesis through cell-autonomous and non-autonomous mechanism, respectively (Tzeng et al. 2018). Shahnazari et al. demonstrated that CXCR4 deletion in osteoblasts reduces bone mass and alternates bone structure in mice model (Shahnazari et al. 2013). CXCL12 expression has a high proportion in most cells and showed the highest expression in MSCs, while CXCR4 was enriched in LMPP, indicating that CXCL12/CXCR4 signaling pathway played a critical role in regulating the signaling among different cell types to affect osteogenesis.

We identified three subgroups of LMPP. LMPP is a type of intermediate precursor cells that differentiate into B cell precursors. The three subgroups showed distinct expression of hub genes, chemokines, and chemokine receptors as well as differentially enriched pathways. It was speculated that the inflammatory factors such as chemokines may be involved in the formation of LMPP with different characteristics. Chemokines secreted by different types of LMPP further affect immune microenvironment and produce pathogenic microenvironment together interacting with other pathogenic factors.

However, this study still has some limitations requiring further clarification. Osteoporosis samples were limited in the original datasets, which may result in false positive outcomes, especially in the development of co-expression networks using WGCNA. Here, we used mature algorithm to remove batch effects and combined different microarray datasets into one dataset with enough osteoporosis samples for analysis, but different origins/tissues of three datasets may still affect the accuracy of the integration and the results. Moreover, only one osteoporosis sample with single-cell sequencing data could be obtained from public databases, and no control samples were included in single-cell data, which might lower the reliability of our conclusions. In addition, we did not consider other factors such as ages, genders, or smoking in osteoporosis pathogenesis. Although we identified 12 hub genes closely involved in the pathogenesis of osteoporosis, further experiments on more clinical samples are needed. Nevertheless, our study delineated a new direction for studying the mechanism of osteoporosis pathogenesis.

## Conclusions

In conclusion, this study explored the relation between immune microenvironment and the pathogenesis of osteoporosis. Our findings could help further understand the mechanisms of unbalanced bone remodeling, providing a direction for developing new therapeutic drugs for osteoporosis patients.

**Abbreviations** *BMD*: Body mineral density; *CDKN1A*: Cyclin-dependent kinase inhibitor 1A; *ES*: Enrichment score; *FDA*: The Food and Drug Administration; *GEO*: Gene Expression Omnibus; *GO*: Gene ontology; *ICAMI*: Intercellular adhesion molecule-1; *ISM*: Indolent systemic mastocytosis; *KEGG*: Kyoto Encyclopedia of Genes and Genomes; *LMPP*: Lymphoid-primed multipotent progenitor; *M-CSF*: Macrophage colony-stimulating factor; *MSCs*: Mesenchymal stem cells; *NLRP3*: Pyrin domain containing protein 3; *PC*: Principle component; *PCA*: Principle component analysis; *QC*: Quality control; *scRNA-seq*: Single-cell RNA sequencing; *Th*: T helper; *WGCNA*: Weighted gene correlation network analysis

**Supplementary Information** The online version contains supplementary material available at <https://doi.org/10.1007/s10142-023-01116-x>.

**Author contribution** ZZ and QK contributed to conception and design. Q Kong contributed to administrative support. ZH and Haider contributed to provision of study materials or patients. ZZ and YL collected and processed the data. All authors read and approved the final manuscript.

**Funding** This work was funded by the Science and technology plan project of Tibet Autonomous Region (No. XZ202201ZY0039G).

**Data availability** The datasets generated and/or analyzed during the current study are openly and permanently available in the [GSE35959] repository, [<https://www.ncbi.nlm.nih.gov/geo/query/acc.cgi?acc=GSE35959>]; in the [GSE7158] repository, [<https://www.ncbi.nlm.nih.gov/geo/query/acc.cgi?acc=GSE7158>]; in the [GSE13850] repository, [<https://www.ncbi.nlm.nih.gov/geo/query/acc.cgi?acc=GSE13850>].

## Declarations

**Ethics approval and consent participate** Not applicable.

**Animal ethics** Not applicable.

**Consent for publication** Not applicable.

**Conflict of interest** The authors declare no competing interests.

## References

- Akkawi I, Zmerly H (2018) Osteoporosis: current concepts. *Joints* 6:122–127. <https://doi.org/10.1055/s-0038-1660790>
- Binder NB, Niederreiter B, Hoffmann O et al (2009) Estrogen-dependent and C-C chemokine receptor-2-dependent pathways determine osteoclast behavior in osteoporosis. *Nat Med* 15:417–424. <https://doi.org/10.1038/nm.1945>
- Brumsen C, Papapoulos SE, Lentjes EG, Kluijn PM, Hamdy NA (2002) A potential role for the mast cell in the pathogenesis of idiopathic

- osteoporosis in men. *Bone* 31:556–561. [https://doi.org/10.1016/s8756-3282\(02\)00875-x](https://doi.org/10.1016/s8756-3282(02)00875-x)
- Brylka LJ, Schinke T (2019) Chemokines in physiological and pathological bone remodeling. *Front Immunol* 10:2182. <https://doi.org/10.3389/fimmu.2019.02182>
- Butler A, Hoffman P, Smibert P, Papalexi E, Satija R (2018) Integrating single-cell transcriptomic data across different conditions, technologies, and species. *Nat Biotechnol* 36:411–420. <https://doi.org/10.1038/nbt.4096>
- Cenci S, Weitzmann MN, Roggia C, Namba N, Novack D, Woodring J, Pacifici R (2000) Estrogen deficiency induces bone loss by enhancing T-cell production of TNF-alpha. *J Clin Invest* 106:1229–1237. <https://doi.org/10.1172/jci11066>
- Chen B, Khodadoust MS, Liu CL, Newman AM, Alizadeh AA (2018) Profiling tumor infiltrating immune cells with CIBERSORT. *Methods Mol Biol* 1711:243–259. [https://doi.org/10.1007/978-1-4939-7493-1\\_12](https://doi.org/10.1007/978-1-4939-7493-1_12)
- Chiappetta N, Gruber B (2006) The role of mast cells in osteoporosis. *Semin Arthritis Rheum* 36:32–36. <https://doi.org/10.1016/j.semarthrit.2006.03.004>
- Collins FL, Williams JO, Bloom AC et al (2017) CCL3 and MMP-9 are induced by TL1A during death receptor 3 (TNFRSF25)-dependent osteoclast function and systemic bone loss. *Bone* 97:94–104. <https://doi.org/10.1016/j.bone.2017.01.002>
- Cummings SR, San Martin J, McClung MR et al (2009) Denosumab for prevention of fractures in postmenopausal women with osteoporosis. *N Engl J Med* 361:756–765. <https://doi.org/10.1056/NEJMoA0809493>
- Dar HY, Singh A, Shukla P, Anupam R, Mondal RK, Mishra PK, Srivastava RK (2018) High dietary salt intake correlates with modulated Th17-Treg cell balance resulting in enhanced bone loss and impaired bone-microarchitecture in male mice. *Sci Rep* 8:2503. <https://doi.org/10.1038/s41598-018-20896-y>
- Diboun I, Wernisch L, Orengo CA, Koltzenburg M (2006) Microarray analysis after RNA amplification can detect pronounced differences in gene expression using limma. *BMC Genomics* 7:252. <https://doi.org/10.1186/1471-2164-7-252>
- Doucet M, Jayaraman S, Swenson E, Tusing B, Weber KL, Kominsky SL (2016) CCL20/CCR6 Signaling regulates bone mass accrual in mice. *J Bone Miner Res* 31:1381–1390. <https://doi.org/10.1002/jbmr.2813>
- Farr JN, Rowsey JL, Eckhardt BA et al (2019) Independent roles of estrogen deficiency and cellular senescence in the pathogenesis of osteoporosis: evidence in young adult mice and older humans. *J Bone Miner Res* 34:1407–1418. <https://doi.org/10.1002/jbmr.3729>
- Fatehi F, Mollahosseini M, Hassanshahi G et al (2017) CC chemokines CCL2, CCL3, CCL4 and CCL5 are elevated in osteoporosis patients. *J Biomed Res* 31:468–470. <https://doi.org/10.7555/jbr.31.20150166>
- Ganguly P, El-Jawhari JJ, Giannoudis PV, Burska AN, Ponchel F, Jones EA (2017) Age-related changes in bone marrow mesenchymal stromal cells: a potential impact on osteoporosis and osteoarthritis development. *Cell Transplant* 26:1520–1529. <https://doi.org/10.1177/0963689717721201>
- Griss J, Viteri G, Sidiropoulos K, Nguyen V, Fabregat A, Hermjakob H (2020) ReactomeGSA - efficient multi-omics comparative pathway analysis. *Mol Cell Proteomics* 19:2115–2125. <https://doi.org/10.1074/mcp.TIR120.002155>
- Han KH, Ryu JW, Lim KE et al (2014) Vascular expression of the chemokine CX3CL1 promotes osteoclast recruitment and exacerbates bone resorption in an irradiated murine model. *Bone* 61:91–101. <https://doi.org/10.1016/j.bone.2013.12.032>
- Imai T, Yasuda N (2016) Therapeutic intervention of inflammatory/immune diseases by inhibition of the fractalkine (CX3CL1)-CX3CR1 pathway. *Inflamm Regen* 36:9. <https://doi.org/10.1186/s41232-016-0017-2>
- Koizumi K, Saitoh Y, Minami T et al (2009) Role of CX3CL1/fractalkine in osteoclast differentiation and bone resorption. *J Immunol* 183:7825–7831. <https://doi.org/10.4049/jimmunol.0803627>
- Komori T (2006) Regulation of osteoblast differentiation by transcription factors. *J Cell Biochem* 99:1233–1239. <https://doi.org/10.1002/jcb.20958>
- Kong L, Yang X (2020) Study of Intercellular Adhesion Molecule-1 (ICAM-1) in Bone Homeostasis. *Curr Drug Targets* 21:328–337. <https://doi.org/10.2174/1389450120666190927122553>
- Kong YY, Feige U, Sarosi I et al (1999) Activated T cells regulate bone loss and joint destruction in adjuvant arthritis through osteoprotegerin ligand. *Nature* 402:304–309. <https://doi.org/10.1038/46303>
- Langfelder P, Horvath S (2008) WGCNA: an R package for weighted correlation network analysis. *BMC Bioinforma* 9:559. <https://doi.org/10.1186/1471-2105-9-559>
- Lavigne P, Benderdour M, Lajeunesse D, Shi Q, Fernandes JC (2004) Expression of ICAM-1 by osteoblasts in healthy individuals and in patients suffering from osteoarthritis and osteoporosis. *Bone* 35:463–470. <https://doi.org/10.1016/j.bone.2003.12.030>
- Lavigne P, Benderdour M, Shi Q, Lajeunesse D, Fernandes JC (2005) Involvement of ICAM-1 in bone metabolism: a potential target in the treatment of bone diseases? *Expert Opin Biol Ther* 5:313–320. <https://doi.org/10.1517/14712598.5.3.313>
- Li H, Xiao Z, Quarles LD, Li W (2021) Osteoporosis: mechanism, molecular target and current status on drug development. *Curr Med Chem* 28:1489–1507. <https://doi.org/10.2174/0929867327666200330142432>
- Liao Y, Wang J, Jaehnig EJ, Shi Z, Zhang B (2019) WebGestalt 2019: gene set analysis toolkit with revamped UIs and APIs. *Nucleic Acids Res* 47:W199–w205. <https://doi.org/10.1093/nar/gkz401>
- Liu L, Zhu Q, Wang J, Xi Q, Zhu H, Gu M (2015) Gene expression changes in human mesenchymal stem cells from patients with osteoporosis. *Mol Med Rep* 12:981–987. <https://doi.org/10.3892/mmr.2015.3514>
- Palmqvist P, Lundberg P, Persson E et al (2006) Inhibition of hormone and cytokine-stimulated osteoclastogenesis and bone resorption by interleukin-4 and interleukin-13 is associated with increased osteoprotegerin and decreased RANKL and RANK in a STAT6-dependent pathway. *J Biol Chem* 281:2414–2429. <https://doi.org/10.1074/jbc.M510160200>
- Pathak JL, Bakker AD, Verschuere P, Lems WF, Luyten FP, Klein-Nulend J, Bravenboer N (2015) CXCL8 and CCL20 enhance osteoclastogenesis via modulation of cytokine production by human primary osteoblasts. *PLoS One* 10:e0131041. <https://doi.org/10.1371/journal.pone.0131041>
- Pei G, Chen L, Zhang W (2017) WGCNA application to proteomic and metabolomic data analysis. *Methods Enzymol* 585:135–158. <https://doi.org/10.1016/bs.mie.2016.09.016>
- Qaseem A, Forciea MA, McLean RM et al (2017) Treatment of low bone density or osteoporosis to prevent fractures in men and women: a clinical practice guideline update from the American College of Physicians. *Ann Intern Med* 166:818–839. <https://doi.org/10.7326/m15-1361>
- Qiu X, Mao Q, Tang Y, Wang L, Chawla R, Pliner HA, Trapnell C (2017) Reversed graph embedding resolves complex single-cell trajectories. *Nat Methods* 14:979–982. <https://doi.org/10.1038/nmeth.4402>
- Ru B, Wong CN, Tong Y et al (2019) TISIDB: an integrated repository portal for tumor-immune system interactions. *Bioinformatics* 35:4200–4202. <https://doi.org/10.1093/bioinformatics/btz210>
- Shahnazari M, Chu V, Wronski TJ, Nissenson RA, Halloran BP (2013) CXCL12/CXCR4 signaling in the osteoblast regulates the mesenchymal stem cell and osteoclast lineage populations. *Faseb J* 27:3505–3513. <https://doi.org/10.1096/fj.12-225763>

- Snouwaert JN, Nguyen M, Repenning PW et al (2016) An NLRP3 mutation causes arthropathy and osteoporosis in humanized mice. *Cell Rep* 17:3077–3088. <https://doi.org/10.1016/j.celrep.2016.11.052>
- Sözen T, Özışık L, Başaran N (2017) An overview and management of osteoporosis. *Eur J Rheumatol* 4:46–56. <https://doi.org/10.5152/eurjrheum.2016.048>
- Srivastava RK, Dar HY, Mishra PK (2018) Immunoporosis: immunology of osteoporosis-role of T cells. *Front Immunol* 9:657. <https://doi.org/10.3389/fimmu.2018.00657>
- Tzeng YS, Chung NC, Chen YR, Huang HY, Chuang WP, Lai DM (2018) Imbalanced osteogenesis and adipogenesis in mice deficient in the chemokine Cxcl12/Sdf1 in the bone mesenchymal stem/progenitor cells. *J Bone Miner Res* 33:679–690. <https://doi.org/10.1002/jbmr.3340>
- van der Veer E, van der Goot W, de Monchy JG, Kluijn-Nelemans HC, van Doormaal JJ (2012) High prevalence of fractures and osteoporosis in patients with indolent systemic mastocytosis. *Allergy* 67:431–438. <https://doi.org/10.1111/j.1398-9995.2011.02780.x>
- Wan H, Qian TY, Hu XJ, Huang CY, Yao WF (2018) Correlation of serum CCL3/MIP-1 $\alpha$  levels with disease severity in postmenopausal osteoporotic females. *Balkan Med J* 35:320–325. <https://doi.org/10.4274/balkanmedj.2017.1165>
- Wang L, Chen K, Wan X, Wang F, Guo Z, Mo Z (2017) NLRP3 inflammasome activation in mesenchymal stem cells inhibits osteogenic differentiation and enhances adipogenic differentiation. *Biochem Biophys Res Commun* 484:871–877. <https://doi.org/10.1016/j.bbrc.2017.02.007>
- Xu L, Zhang L, Wang Z et al (2018) Melatonin suppresses estrogen deficiency-induced osteoporosis and promotes osteoblastogenesis by inactivating the NLRP3 inflammasome. *Calcif Tissue Int* 103:400–410. <https://doi.org/10.1007/s00223-018-0428-y>
- Yu G, Wang LG, Han Y, He QY (2012) clusterProfiler: an R package for comparing biological themes among gene clusters. *Omics* 16:284–287. <https://doi.org/10.1089/omi.2011.0118>

**Publisher's note** Springer Nature remains neutral with regard to jurisdictional claims in published maps and institutional affiliations.

Springer Nature or its licensor (e.g. a society or other partner) holds exclusive rights to this article under a publishing agreement with the author(s) or other rightsholder(s); author self-archiving of the accepted manuscript version of this article is solely governed by the terms of such publishing agreement and applicable law.